Spin-Dependent Terms of the Breit-Pauli Hamiltonian Evaluated with an Explicitly Correlated Gaussian Basis Set for Molecular **Computations**

Péter Jeszenszki, Péter Hollósy, Adám Margócsy, and Edit Mátyus*



Cite This: https://doi.org/10.1021/acsphyschemau.5c00055



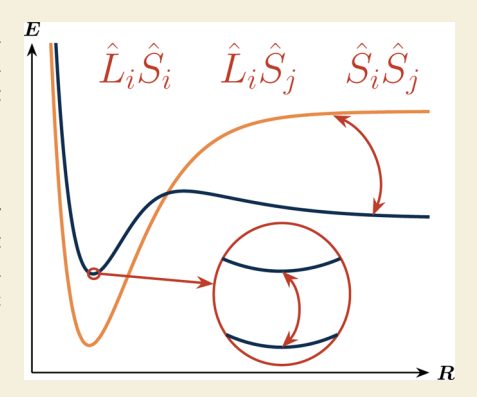
ACCESS I

III Metrics & More

Article Recommendations

Supporting Information

ABSTRACT: This work collects the spin-dependent leading-order relativistic and quantum-electrodynamical corrections for the electronic structure of atoms and molecules within the nonrelativistic quantum electrodynamics framework. We report the computation of perturbative corrections using an explicitly correlated Gaussian basis set, which allows high-precision computations for few-electron systems. In addition to numerical tests for triplet Be, triplet H₂, and triplet H₃ states and comparison with nopair Dirac-Coulomb-Breit Hamiltonian energies, numerical results are reported for electronically excited states of the helium dimer, He2, for which the present implementation delivers high-precision magnetic coupling curves necessary for a quantitative understanding of the fine structure of its high-resolution rovibronic spectrum.



KEYWORDS: spin-orbit coupling, spin-spin coupling, Breit-Pauli Hamiltonian, explicitly correlated Gaussian, triplet H_{2j} triplet H_{2j} triplet H₃⁺

1. INTRODUCTION

Few-electron atoms and molecules are sometimes referred to as "calculable" systems, which allow to extensively test and extend the frontier of current methodologies and probe small physical effects by comparison with high-resolution spectroscopy experiments. At the extreme of precision physics applications, the most accurate experimental and most possible complete theoretical treatments for ionization, dissociation and rovibrational energies progress head-to-head, 1-3 and ultimately deliver more precise values for fundamental physical constants and set bounds on possible new types of forces.^{4,5} Furthermore, the reliable identification of quantum states is crucial for the manipulation of atoms and molecules with laser light, which contributes to advancements in the field of ultracold molecules⁶ and quantum technologies.^{7,8} Theoretical and computational progress in precision physics delivers benchmark values for quantum chemistry methods targeting larger systems.

For few-particle systems, an explicitly correlated basis set is frequently used in combination with a variational procedure to capture the essential electron-electron correlation effects, leading to fast convergence in the energy and other physical properties. 9,10 To obtain analytic expressions for the matrix elements, floating explicitly correlated Gaussians (fECGs) are used as a spatial basis set, ⁹⁻¹³ for which numerical efficiency in the high-precision computation of few-electron systems has already been demonstrated. $^{14-27}$

Since the electronic energy of few-particle systems can be converged to high precision in a variational fECG approach, the relativistic and quantum electrodynamical (QED) contributions become "visible" and important even for (compounds of) light elements. High-resolution spectroscopic measurements reveal small magnetic effects, seen as fine and hyperfine splittings in the spectra. We will refer to the relevant interactions as "spin-dependent" relativistic (and QED) interactions, and we will also use the term "spin-independent" relativistic and QED corrections, which contribute to the centroid energy (defined as the average of the fine-structure energy levels corresponding to the degenerate nonrelativistic subspace). While the computation of the centroid corrections is well elaborated, including the regularisation techniques, ²⁸⁻³⁰ which enhance the convergence of singular terms in the Gaussian basis representation (for the incorrect electronnucleus and electron-electron coalescence behavior).

In this paper, we focus on an fECG-based implementation of the spin-dependent matrix elements of the Breit-Pauli Hamiltonian. We also include corrections for the anomalous

Received: June 23, 2025 Revised: September 9, 2025 Accepted: September 9, 2025



magnetic moment of the electron, which constitutes the leading-order ($\alpha^3 E_{\rm h}$, with the α fine-structure constant) QED corrections to the spin-dependent terms. We note that higher-order QED ($\alpha^4 E_{\rm h}$) corrections have been derived by Douglas and Kroll in 1974 for the helium atom triplet states³¹ and more recently, the $\alpha^5 E_{\rm h}$ -order corrections have been derived and evaluated for triplet helium states. Inner shell transitions are in excellent agreement with experiment, though there is a significant deviation for the ionization energy between theory 33,34 and experiment.

The present work focuses on the relativistic and leading-order QED corrections, i.e., up to $\alpha^3 E_{\rm h}$ order, but goes beyond atomic applications; molecular systems with clamped nuclei require the development of a floating ECG methodology, reported in the present work.

Nonfloating, spherically symmetric, ECG basis sets have already been successfully used in spin-dependent atomic computations, considering beryllium, boron and carbon atomic states. ^{19,39–43} By relaxing the Born–Oppenheimer approximation, small molecules (H₂, ^{44,45} HD, ⁴⁶ BH and BH, have also been computed (with varying precision). However, these approaches cannot be applied directly to clamped nuclei and molecular computations exploiting the Born–Oppenheimer approximation, which would otherwise be advantageous, since the computational complexity grows rapidly with the number of particles.

In this paper, we report a general N-electron implementation without restrictions on the number and spatial arrangement of the clamped atomic nuclei. The implementation is based on a spinor basis representation, in which the spatial and spin components are evaluated independently and subsequently combined via calculating simple tensor products. The approach is, in principle, "general" and not restricted by the number of electrons or point-group symmetry. For testing the developed methodology and computer implementation, we perform computations for triplet Be for comparison with literature values. As to molecular systems (the main target of this work), two-electron triplet H₂ and also two-electron triplet H₃ (both a linear and a triangular configuration) are also included in the test set. For molecular systems, high-accuracy benchmark values are not available in the literature; so, we tested these results with our in-house developed no-pair Dirac-Coulomb-Breit methodology (currently available for two-spin-1/2fermion systems), as in which the spin-dependent Breit—Pauli relativistic effects appear at lowest order of the fine-structure constant. Then, as a first large-scale application of the implementation, motivated by recent and ongoing experiments, ⁴⁹⁻⁵¹ we compute magnetic coupling curves for several electronically excited states of the (triplet and singlet) He2 molecule, which significantly improve upon previously available quantum chemistry computations. 52-58 The newly computed coupling curves are used in rovibronic-fine-structure computations reported in separate papers.^{26,7}

2. THEORETICAL FRAMEWORK

For atoms and molecules with low nuclear charge, the nonrelativistic description often provides a good starting point. The nonrelativistic electronic energy is incremented with relativistic and QED corrections arranged according to powers of the α fine-structure constant. In this paper, we include all terms up to α^3 (in Hartree atomic units)

$$E = E^{(0)} + \alpha^2 E^{(2)} + \alpha^3 E^{(3)} \tag{1}$$

We start by solving the Schrödinger equation

$$\hat{H}^{(0)}|\varphi^{(0)}\rangle = E^{(0)}|\varphi^{(0)}\rangle \tag{2}$$

for the nonrelativistic electronic Hamiltonian

$$\hat{H}^{(0)} = -\frac{1}{2} \sum_{i=1}^{n_{el}} \Delta_{r_i} - \sum_{i=1}^{n_{el}} \sum_{A=1}^{N_{nuc}} \frac{Z_A}{r_{iA}} + \sum_{i=1}^{n_{el}} \sum_{j>i}^{n_{el}} \frac{1}{r_{ij}}$$
(3)

with the nuclei clamped at the R_A ($A = 1,..., N_{\text{nuc}}$) positions. We use the short notation, $r_{iX} = |r_{iX}|$, where X is either a nucleus or an electron index, i.e., resulting in $r_{iA} = r_i - R_A$ or $r_{ij} = r_i - r_j$.

The leading-order relativistic corrections, $\alpha^2 E^{(2)}$, can be computed as the expectation value of the Breit–Pauli (BP) Hamiltonian with the nonrelativistic wave function, $\varphi^{(0)}$. The focus of this work is the computation of the spin-dependent contributions, so we write the Hamiltonian as the sum of spin-independent (sn) and spin-dependent (sd) terms ^{59,60}

$$\begin{split} \hat{H}^{(2)} &= \hat{H}_{\rm sn}^{(2)} + \hat{H}_{\rm sd}^{(2)} \\ &= \hat{H}_{\rm MV} + \hat{H}_{\rm D1} + \hat{H}_{\rm OO} + \hat{H}_{\rm D2} + \hat{H}_{\rm SO} + \hat{H}_{\rm SOO} \\ &+ \hat{H}_{\rm SOO'} + \hat{H}_{\rm SS} \end{split} \tag{4}$$

where the manifestly spin-independent terms are reiterated only for completeness, i.e., the mass-velocity (MV), the oneelectron Darwin (D1), the two-electron Darwin (D2), and the orbit—orbit terms (OO) are

$$\hat{H}_{MV} = -\frac{1}{8} \sum_{i=1}^{n_{el}} (\hat{p}_i^2)^2, \qquad \hat{H}_{D1} = \frac{\pi}{2} \sum_{i=1}^{n_{el}} \sum_{A=1}^{N_{nuc}} Z_A \delta(\mathbf{r}_{iA}),$$

$$\hat{H}_{D2} = -\pi \sum_{i=1}^{n_{el}} \sum_{j>i}^{n_{el}} \delta(\mathbf{r}_{ij})$$
(5)

and

$$\hat{H}_{OO} = -\frac{1}{2} \sum_{i=1}^{n_{el}} \sum_{j>i}^{n_{el}} \left[\frac{1}{r_{ij}} \hat{\mathbf{p}}_{i} \hat{\mathbf{p}}_{j} + \frac{1}{r_{ij}^{3}} (\mathbf{r}_{ij} (\mathbf{r}_{ij} \hat{\mathbf{p}}_{j}) \hat{\mathbf{p}}_{i}) \right]$$
(6)

respectively. The corrections carrying spin operators in their expressions are the spin-orbit interaction, with $\hat{\bf l}_{iX}={\bf r}_{iX}\times\hat{\bf p}_i$ and $\hat{\bf s}_i=\frac{1}{2}I(1)\otimes\ldots\otimes {\bf \sigma}(i)\otimes\ldots\otimes I(n_{\rm el})$ with the ${\bf \sigma}=(\sigma_{x},\sigma_y,\sigma_z)$ Pauli matrices

$$\hat{H}_{SO} = \frac{1}{2} \sum_{i=1}^{n_{el}} \sum_{A=1}^{N_{nuc}} \frac{Z_A}{r_{iA}^3} \hat{\mathbf{s}}_i \hat{\mathbf{l}}_{iA}$$
 (7)

the spin-own-orbit interaction

$$\hat{H}_{SOO} = -\frac{1}{2} \sum_{i=1}^{n_{el}} \sum_{j>i}^{n_{el}} \frac{1}{r_{ij}^3} [\hat{s}_i \hat{l}_{ij} + \hat{s}_j \hat{l}_{ji}]$$
(8)

the spin-other-orbit interaction

$$\hat{H}_{SOO'} = -\sum_{i=1}^{n_{el}} \sum_{j>i}^{n_{el}} \frac{1}{r_{ij}^3} [\hat{s}_i \hat{l}_{ji} + \hat{s}_j \hat{l}_{ij}]$$
(9)

and the spin-spin interaction

$$\hat{H}_{SS} = \sum_{i=1}^{n_{el}} \sum_{j>i}^{n_{el}} \left[(\hat{\mathbf{s}}_i \hat{\mathbf{s}}_j) \left(\hat{\mathbf{p}}_i \hat{\mathbf{p}}_j \frac{1}{r_{ij}} \right) - (\hat{\mathbf{s}}_i \hat{\mathbf{p}}_j) \left(\hat{\mathbf{s}}_j \hat{\mathbf{p}}_i \frac{1}{r_{ij}} \right) \right]$$

$$= \hat{H}_{SS,dp} + \hat{H}_{SS,c}$$
(10)

which is written as the sum of the magnetic spin dipole—dipole interaction

$$\hat{H}_{SS,dp} = \sum_{i=1}^{n_{el}} \sum_{j>i}^{n_{el}} \left[\frac{\hat{s}_i \hat{s}_j}{r_{ij}^3} - \frac{3(\hat{s}_i r_{ij})(\hat{s}_j r_{ij})}{r_{ij}^5} \right]$$
(11)

and the Fermi contact term for each pair of electrons

$$\hat{H}_{SS,c} = -\frac{8\pi}{3} \sum_{i=1}^{n_{el}} \sum_{j>i}^{n_{el}} \hat{s}_{i} \hat{s}_{j} \delta(\mathbf{r}_{ij}) = -2\pi \sum_{i=1}^{n_{el}} \sum_{j>i}^{n_{el}} \delta(\mathbf{r}_{ij})$$
(12)

where in the last step we used the form of the Fermi contact term over the antisymmetrized Hilbert subspace.

The spin-independent terms, giving rise to the relativistic correction of the "centroid" are collected as

$$\alpha^2 \hat{H}_{\rm sn}^{(2)} = \alpha^2 [\hat{H}_{\rm MV} + \hat{H}_{\rm D1} + \hat{H}_{\rm OO} + \hat{H}_{\rm D2} + \hat{H}_{\rm SS,c}] \tag{13}$$

The precise computation of expectation values (with Gaussian basis sets) for this part has been discussed in detail elsewhere. ^{28–30}

The focus of the present work is the implementation of the spin-dependent terms

$$\alpha^2 \hat{H}_{sd}^{(2)} = \alpha^2 [\hat{H}_{SO} + \hat{H}_{SOO} + \hat{H}_{SOO'} + \hat{H}_{SS,dp}]$$
 (14)

In addition, we consider the effect of the anomalous magnetic moment of the electron $^{61-63}$ on the spin-dependent terms, which gives rise to the leading-order QED correction for the spin-dependent part (a brief summary with references is in the SM of ref 26)

$$\alpha^{3} \hat{H}_{sd}^{(3)} = \alpha^{2} \left[\frac{\alpha}{\pi} \hat{H}_{SO} + \frac{\alpha}{\pi} \hat{H}_{SOO} + \frac{1}{2} \frac{\alpha}{\pi} \hat{H}_{SOO'} + \frac{\alpha}{\pi} \hat{H}_{SS,dp} \right]$$
(15)

So, up to $\alpha^3 E_h$ order, the spin-dependent terms are

$$\alpha^{2} \hat{H}_{sd} = \alpha^{2} \left[\left(1 + \frac{\alpha}{\pi} \right) \hat{H}_{SO} + \left(1 + \frac{\alpha}{\pi} \right) \hat{H}_{SOO} + \left(1 + \frac{\alpha}{\pi} \right) \hat{H}_{SS,dp} \right]$$

$$+ \left(1 + \frac{\alpha}{2\pi} \right) \hat{H}_{SOO'} + \left(1 + \frac{\alpha}{\pi} \right) \hat{H}_{SS,dp}$$
(16)

3. METHODS AND IMPLEMENTATION

For the numerical implementation, the nonrelativistic wave function is expanded in an explicitly correlated basis set

$$|\varphi^{(\Gamma,SM_S)}\rangle = \sum_{\mu=1}^{N} C_{\mu} |\phi_{\mu}^{(\Gamma,SM_S)}\rangle \tag{17}$$

where the coefficients C_{μ} are obtained by diagonalizing the nonrelativistic Hamiltonian matrix. We define the basis function as

$$\phi_{\mu}^{(\Gamma,SM_S)} = \phi^{(\Gamma,SM_S)}(\mathbf{r}; \mathbf{A}_{\mu}, \mathbf{s}_{\mu}, \mathbf{\theta}_{\mu}) = \hat{\mathcal{A}}\{f^{(\Gamma)}(\mathbf{r}; \mathbf{A}_{\mu}, \mathbf{s}_{\mu})\chi^{(SM_S)}(\mathbf{\theta}_{\mu})\}$$
(18)

 $\chi^{(\mathrm{SM_S})}(\theta_\mu)$ is a spin function, $f^{(\Gamma)}(r;A_\mu s_\mu)$ is a spatial function. In this work, symmetrized floating explicitly correlated Gaussian functions (fECG) $^{9-13}$ are used as spatial functions

$$f_{\mu}^{(\Gamma)} = f^{(\Gamma)}(\mathbf{r}; \mathbf{A}_{\mu}, \mathbf{s}_{\mu}) = \hat{\mathcal{P}}_{\Gamma} \exp[-(\mathbf{r} - \mathbf{s}_{\mu})^{\mathrm{T}} (\mathbf{A}_{\mu} \otimes \mathbf{I}_{3})(\mathbf{r} - \mathbf{s}_{\mu})]$$

$$\tag{19}$$

where \hat{P}_{Γ} is the projector onto the Γ irreducible representation (irrep) of the point-group defined by the fixed nuclear skeleton (technical details are reported in some detail in the Supporting Information of ref 48), I_3 is the three-dimensional identity matrix, A_{μ} and s_{μ} are nonlinear parameters, which are generated and optimized by minimization of the nonrelativistic energy. 9,10,26,64,65

 $\hat{\mathcal{A}}$ is the antisymmetrization operator for the electrons

$$\hat{\mathcal{A}} = (N_{\text{perm}})^{-1/2} \sum_{r=1}^{N_{\text{perm}}} (-1)^{p_r} \hat{P}_r \hat{Q}_r$$
(20)

where the sum is over all permutations $(N_{\text{perm}} = n_{\text{el}}!)$, p_r is the parity (odd or even) of the permutation r, and \hat{P}_r and \hat{Q}_r are the permutation operators acting on the spatial (r) and the spin (σ) degrees of freedom, respectively. We note the quasi-idempotency of the antisymmetrizer, $\hat{\mathcal{H}}^2 = (N_{\text{perm}})^{\frac{1}{2}}\hat{\mathcal{H}}$.

Regarding the spin function $\chi_{\mu}^{(SM_S)} = \chi^{(SM_S)}(\boldsymbol{\theta}_{\mu})$, S is the total electron spin quantum number and M_S is the quantum number for the spin projection. S, M_S for $n_{\rm el}$ electrons define a spin subspace, for which the spin functions can be expressed as a linear combination of the elementary spin functions; we call this representation the θ -parametrization 9,64 (see also Supporting Information). In the nonrelativistic energy minimization, we also include the $\boldsymbol{\theta}_{\mu}$ parameter vector.

Next, let us consider a general, permutationally invariant operator written as a linear combination (in terms of electronic and Cartesian indexes) of products of \hat{G}_{ia} spatial and \hat{T}_{ia} spin-dependent factors

$$\hat{\mathcal{H}} = \sum_{i=1}^{n_{\text{el}}} \sum_{a=1}^{3} \hat{G}_{ia} \hat{T}_{ia}$$
(21)

We compute matrix elements of this operator with nonrelativistic electronic functions, $\varphi=\varphi^{(\Gamma,SM_{\rm S})}$ and $\varphi'=\varphi^{(\Gamma',S'M_{\rm S}')}$ as

$$\begin{split} \langle \varphi | \hat{\mathcal{H}} | \varphi' \rangle &= \sum_{\mu=1}^{N} \sum_{\nu=1}^{N'} C_{\mu}^{*} C_{\nu}^{\prime} \langle \phi_{\mu} | \hat{\mathcal{H}} | \phi_{\nu}^{\prime} \rangle \\ &= \sum_{\mu=1}^{N} \sum_{\nu=1}^{N'} C_{\mu}^{*} C_{\nu}^{\prime} \langle \hat{\mathcal{A}} \{ f_{\mu} \chi_{\mu} \} | \hat{\mathcal{H}} | \hat{\mathcal{A}} \{ f_{\nu}^{\prime} \chi_{\nu}^{\prime} \} \rangle \\ &= \sum_{\mu=1}^{N} \sum_{\nu=1}^{N'} C_{\mu}^{*} C_{\nu}^{\prime} \sum_{r=1}^{N_{\text{perm}}} (-1)^{p_{r}} \langle f_{\mu} \chi_{\mu} | \hat{\mathcal{H}} | (\hat{P}_{r} f_{\nu}^{\prime}) (\hat{Q}_{r} \chi_{\nu}^{\prime}) \rangle \\ &= \sum_{\mu=1}^{N} \sum_{\nu=1}^{N'} C_{\mu}^{*} C_{\nu}^{\prime} \sum_{r=1}^{N_{\text{perm}}} (-1)^{p_{r}} \cdot \sum_{r=1}^{N_{\text{perm}}} \sum_{n=1}^{N_{\text{el}}} \langle f_{\mu} | \hat{G}_{id} | \hat{P}_{r} f_{\nu}^{\prime} \rangle_{r} \langle \chi_{\mu} | \hat{T}_{id} | \hat{Q}_{r} \chi_{\nu}^{\prime} \rangle_{\sigma} \end{split}$$

The irreducible representation of spatial symmetry can differ for f_{μ} and f'_{ν} , hence, the spatial-symmetry operations are retained in the bra and the ket functions. For the computation of the spin-orbit (SO), the spin-own-orbit (SOO), and the spin-other-orbit (SOO') terms, eqs 7–9, the \hat{G}_{ia} factors are

SO:
$$\hat{G}_{ia}^{SO} = \frac{1}{2} \sum_{A=1}^{N_{\text{nuc}}} \frac{Z_A}{r_{iA}^3} \hat{l}_{iA,a}$$
 (23)

SOO:
$$\hat{G}_{ia}^{SOO} = -\frac{1}{4} \sum_{j \neq i}^{n_{el}} \frac{1}{r_{ij}^3} \hat{I}_{ij,a}$$
 (24)

SOO':
$$\hat{G}_{ia}^{SOO'} = -\frac{1}{2} \sum_{j \neq i}^{n_{el}} \frac{1}{r_{ij}^3} \hat{l}_{ji,a}$$
 (25)

and the \hat{T}_{ia} factor is simply the spin matrix

$$\hat{T}_{ia} = \hat{s}_{ia} \tag{26}$$

The spin—spin dipolar term, eq 11, is a two-electron term, and by analogous calculation to eq 22, we obtain

$$\langle \varphi | \hat{H}_{SS,dp} | \varphi' \rangle = \sum_{\mu=1}^{N} \sum_{\nu=1}^{N'} C_{\mu}^{*} C_{\nu}^{'} \sum_{r=1}^{N_{perm}} (-1)^{p_{r}}$$

$$\sum_{i=1}^{n_{el}} \sum_{j>i}^{n_{el}} \sum_{a,b=1}^{3} \langle f_{\mu} | \hat{G}_{ij,ab} | \hat{P}_{r} f_{\nu}^{'} \rangle_{r} \langle \chi_{\mu} | \hat{s}_{ia} \hat{s}_{jb} | \hat{Q}_{r} \chi_{\nu}^{'} \rangle_{\sigma}$$
(27)

where

$$\hat{G}_{ij,ab} = \frac{\delta_{ab}}{r_{ij}^3} - \frac{3r_{ij,a}r_{ij,b}}{r_{ij}^5}$$
(28)

The spatial integrals are calculated analytically by exploiting the mathematical properties of fECGs, similarly to our previous work, e.g., refs 17, 20, and 66-68.

Since the present work is about the evaluation of the spin-dependent Breit-Pauli matrix elements, some notes regarding the spinor structure and matrix elements are appropriate. To evaluate the spin matrix elements, the spin-adapted θ -parametrization (see also refs 25 and 26) is transformed into the spinor (vector) representation (see also Supporting Information)

$$|\chi_{\mu}^{(SM_S)}(\boldsymbol{\theta})\rangle = \sum_{t_1, t_2, \dots, t_{n_{el}}} d_{t_1 t_2 \dots t_{n_{el}}, \mu}^{(SM_S)} |\Xi_{t_1 t_2 \dots t_{n_{el}}}\rangle$$

$$\Sigma_{t_i} = 2M_S + 1$$
(29)

where $t_i=2m_{s_i}+1$, $|\Xi_{t_1t_2...t_{n_{\rm el}}}\rangle=|\eta_{t_1}\rangle\otimes|\eta_{t_2}\rangle\otimes\ldots\otimes|\eta_{t_{n_{\rm el}}}\rangle$, and $|\eta_{t_i}\rangle$ is a single-particle spin function (vector). Depending on the $m_{s_i}=+\frac{1}{2}$ or $-\frac{1}{2}$ value, the spin function is "spin up", $|\eta_1\rangle=|\alpha\rangle=\left(\frac{1}{0}\right)$, or "spin down", $|\eta_0\rangle=|\beta\rangle=\left(\frac{0}{1}\right)$.

Then, the \hat{s}_i spin operator is represented as the tensor product of (two-by-two) identity matrices and the Pauli matrix

$$\mathbf{s}_{ia} = \frac{\hbar}{2} \mathbf{I}(1) \otimes \mathbf{I}(2) \dots \mathbf{I}(i-1) \otimes \mathbf{\sigma}_{a}(i) \otimes \mathbf{I}(i+1) \dots \otimes \mathbf{I}(n_{el})$$
(30)

The matrix representation of the $\hat{s}_{ia}\hat{s}_{jb}$ operator is obtained as $s_{ia}s_{jb}$ (the spin space is complete), and

$$\mathbf{s}_{ia}\mathbf{s}_{jb} = \frac{\hbar}{2}\mathbf{I}(1) \otimes \ldots \otimes \mathbf{\sigma}_{a}(i) \otimes \ldots \otimes \mathbf{\sigma}_{b}(j) \otimes \ldots \otimes \mathbf{I}(n_{\mathrm{el}}),$$

$$i \neq j \tag{31}$$

$$\mathbf{s}_{ia}\mathbf{s}_{ib} = \frac{\hbar}{2}\mathbf{I}(1) \otimes \ldots \otimes \mathbf{\sigma}_{a}\mathbf{\sigma}_{b}(i) \otimes \ldots \otimes \mathbf{I}(n_{el})$$
(32)

Then, the matrix elements of the spin functions are written as (where the tensor structure can be further exploited)

$$\langle \chi_{\mu} | \hat{\mathbf{s}}_{ia} | \chi_{\nu}' \rangle_{\sigma} = \langle \chi_{\mu}^{(\mathrm{SM}_{\mathrm{S}})} | \hat{\mathbf{s}}_{ia} | \chi_{\nu}^{(\mathrm{S'M}_{\mathrm{S}}')} \rangle_{\sigma} = \mathbf{d}_{\mu}^{(\mathrm{SM}_{\mathrm{S}})^{\dagger}} \mathbf{s}_{ia} \mathbf{d}_{\nu}^{(\mathrm{S'M}_{\mathrm{S}}')}$$

$$(33)$$

$$\langle \chi_{\mu} | \hat{\mathbf{s}}_{ia} \hat{\mathbf{s}}_{jb} | \chi_{\nu}' \rangle_{\sigma} = \langle \chi_{\mu}^{(\mathrm{SM}_{\mathrm{S}})} | \hat{\mathbf{s}}_{ia} \hat{\mathbf{s}}_{jb} | \chi_{\nu}^{(\mathrm{S'M}_{\mathrm{S}}')} \rangle_{\sigma} = \mathbf{d}_{\mu}^{(\mathrm{SM}_{\mathrm{S}}) \dagger} \mathbf{s}_{ia} \mathbf{s}_{jb} \mathbf{d}_{\nu}^{(\mathrm{S'M}_{\mathrm{S}}')}$$
(34)

In a nutshell, the following algorithm has been implemented in our in-house developed fECG-based computer program, named QUANT-EN, to compute matrix elements of spin-dependent relativistic operators connecting various electronic-spin states of small molecules (and also atoms, of course):

- 1. The nonrelativistic energies and wave functions are determined by the nonlinear optimization of the A_{μ} , s_{μ} , and θ_{μ} parameters and diagonalization of the Hamiltonian for a specific spin state, e.g., $M_{\rm S}=0$.
- 2. The spin function $\chi_{\mu}^{(\mathrm{SM}_{\mathrm{S}})}$ with parameters $\boldsymbol{\theta}_{\mu}$ are transformed to the spinor (vector) representation, eq 29, to obtain the $d_{\mathfrak{t}_{1}\mathfrak{t}_{2}...\mathfrak{t}_{n_{\mathrm{cl}}},\mu}^{(\mathrm{SM}_{\mathrm{S}})}$ coefficients.
- 3. The spin operators (matrices) s_i are constructed according to eq 30, and the ladder operators (matrices) are generated as

$$s_i^{\pm} = s_{i,x} \pm i s_{i,y},$$
 $S^{\pm} = \sum_{i=1}^{n_{el}} s_i^{\pm}$ (35)

Then, the target $M_{\rm S}$ states are obtained by matrix-vector multiplication

$$\mathbf{d}_{\mu}^{(S,M_{S}\pm 1)} = \mathbf{S}^{\pm} \mathbf{d}_{\mu}^{(SM_{S})} \tag{36}$$

- 4. The spatial matrix elements, $\langle f_{\mu}^{(\Gamma)}|\hat{G}_{ia}^{x}|\hat{P}_{r}f_{\nu}^{(\Gamma')}\rangle_{r}$ (x = SO, SOO, SOO') and $\langle f_{\mu}^{(\Gamma)}|\hat{G}_{ij,ab}^{SS}|\hat{P}_{r}f_{\nu}^{(\Gamma')}\rangle_{r}$ (SS,dp), are computed using the analytic fECG integral expressions.
- The spatial and spin contributions are combined according to eqs 22 and 27, to obtain the relativistic (and QED) coupling matrix elements of the electron-spin states.

4. NUMERICAL TESTS OF THE IMPLEMENTATION

This section presents numerical examples used to test the computer implementation of the spin-dependent Breit–Pauli Hamiltonian (BP) matrix elements. For the (atomic) test systems, relatively small basis sets are used, which can be readily extended for better-converged results (if required). The value $\alpha^{-1}=137.035999177$, recommended by CODATA 2022, ⁶⁹ is used in all computations.

4.1. Atomic Test System

For the spherically symmetric (atomic) case, there are high-accuracy ECG implementations already available in the literature, including the analytic angular prefactor corresponding to higher angular momentum states. ^{39–41} As a first test case of our implementation, intended for the more general molecular problem, we computed the spin-dependent BP matrix elements of the 2 ³P° state of the Be atom. We computed the expectation value of the spin-dependent BP operator terms, eq 14, labeled as $\langle \hat{H}_X \rangle_J (X = \text{SO,SOO} \otimes \text{SOO}', \text{SS,dp})$ with the $M_J = 0$ wave function (Table 1). The relative error due to the finite basis size is approximately the same for all three terms; the deviations from the reference values are attributed to the incompleteness of our basis set. We also note

Table 1. Be 2 ³P° State: Testing the Implementation of the Spin-Dependent Breit-Pauli Matrix Elements^a

N	$E^{(0)}$	$\alpha^2 \langle \hat{H}_{\rm SO} \rangle_0$	$\alpha^2 \langle \hat{H}_{\rm SOO} + \hat{H}_{\rm SOO'} \rangle_0$	$\alpha^2 \langle \hat{H}_{SS,dp} \rangle_0$
5	-14.44	-24	17.8	1.337
10	-14.54	-28	20.6	1.363
20	-14.553	-30.4	21.76	1.439
30	-14.5612	-31.60	22.141	1.378
50	-14.56514	-32.06	22.288	1.372
100	-14.56669	-32.18	22.278	1.367
ref 41	-14.567244230	-32.2416	22.2450	1.365

^aThe non-relativistic energy, $E^{(0)}$ in $E_{\rm h}$, and the expectation value of spin-dependent operators for the $M_{\rm J}=0$ state in $\mu E_{\rm h}$, are given as a function of the number of ECG functions, N.

Table 2. H_2 a $^3\Sigma_g^+$ and b $^3\Sigma_u^+$ States (R=1.4 bohr): The Non-relativistic Energy, $E^{(0)}$ in E_h , and the Zero-Field Splitting, ΔE in μE_h^a

		$H_2 \ a^{\ 3}\Sigma_g^+$			$H_2\;b^{\;3}\Sigma_u^+$	
N	$E^{(0)}$	$\Delta E^{ m BP}$	$\Delta E^{ m DCB}$	$E^{(0)}$	$\Delta E^{ m BP}$	$\Delta E^{ m DCB}$
10	-0.713250	-0.0061	-0.0061	-0.7815	3.16	3.16
20	-0.713553	0.0139	0.0139	-0.7833	3.13	3.13
30	-0.713602	0.0199	0.0199	-0.784121	3.0403	3.0402
50	-0.713635	0.02145	0.02145	-0.784227	3.0329	3.0329
100	-0.71364021	0.02231	0.02231	-0.7842435	3.03109	3.03105
150	-0.71364046	0.022345	0.022345	-0.78424414	3.03089	3.03084
ref 72	-0.7130	0.02		-0.7840	3.056	

^aFor the perturbative correction $\Delta E^{\rm BP} = \alpha^2 \Delta E^{(2)} = \alpha^2 [E_0^{(2)} - E_{\pm 1}^{(2)}] = \alpha^2 [\langle H_{\rm SS,dp} \rangle_0 - \langle H_{\rm SS,dp} \rangle_{\pm 1}]$ as a function of the number of fECGs, N. The DCB superscript labels the no-pair DCB results.

Table 3. Triplet H₃⁺ Ground State: The Non-relativistic Energy, $E^{(0)}$ in $E_{\rm h}$, and the Zero-Field Splitting, ΔE in $\mu E_{\rm h}$, as a Function of the Number of fECGs, N^a

	linear (ed	quilibrium) struct	ture	triangular structure						
N	E ⁽⁰⁾	$\Delta E^{ m BP}$	$\Delta E^{ m DCB}$	E ⁽⁰⁾	$\Delta E_{21}^{\mathrm{BP}}$	$\Delta E_{21}^{ m DCB}$	$\Delta E_{32}^{\mathrm{BP}}$	$\Delta E_{32}^{\mathrm{DCB}}$		
10	-1.1127	1.781	1.781	-1.097	0.0051	0.0051	0.4602	0.4601		
20	-1.11555	1.794	1.794	-1.1026	0.0063	0.0063	0.45956	0.45954		
30	-1.11596	1.7580	1.7580	-1.1039	0.0069	0.0069	0.45955	0.45953		
50	-1.116086	1.75719	1.75723	-1.10429	0.0074	0.0074	0.45935	0.45933		
70	-1.1161027	1.75736	1.75729	-1.10436	0.00763	0.00763	0.45925	0.45923		
100	-1.1161076	1.75693	1.75686	-1.104391	0.00779	0.00779	0.459152	0.459132		
150	-1.1161088	1.75680	1.75712	-1.1044023	0.007871	0.007871	0.459108	0.459086		
200	-1.11610912	1.75672	1.75665	-1.1044055	0.007878	0.007878	0.459097	0.459075		
ref	-1.1161063^{73}			-1.10408^{74}						

"For the linear (equilibrium) structure, the centres of the fECGs were restricted to the nuclear axis and $R_{\rm pp,1} = R_{\rm pp,2} = 2.454$ bohr. For the general triangular structure, the centres of the fECGs were restricted in the plane of the triangle (without any further point-group symmetry projections), $R_{\rm pp,1} = 1.939$ bohr, $R_{\rm pp,2} = 5.961$ bohr, and $\angle_{\rm ppp} = 64.4^{\circ}$. For the linear (equilibrium) geometry, $\Delta E = E_0 - E_{\pm 1} = \alpha^2 [\langle \hat{H}_{\rm SS,dp} \rangle_0 - \langle \hat{H}_{\rm SS,dp} \rangle_{\pm 1}]$. For the triangular structure, $\Delta E_{ij} = E_i - E_{ji}$ where i and j labels the energy levels (please see also text). The DCB superscript labels the no-pair Dirac-Coulomb-Breit results.

that the expectation value for other $M_J = \pm 1$, ± 2 values of the 2 $^3\mathrm{P}$ spin subspace of this atomic system can be calculated from the $\langle \hat{H}_{\mathrm{Y}} \rangle_0$ matrix elements through known relations, e.g., in ref 40.

4.2. Molecular Applications

Regarding molecular systems within the Born-Oppenheimer approximation, we are not aware of any literature data for the high-precision computation of the spin-dependent BP matrix elements. Still, to be able to test the spin-dependent BP implementation reported in this work, we used our in-house implementation of the high-precision no-pair Dirac-Coulomb-Breit (DCB) approach. 20,21,48,66,67,70 In particular, ref 48 is most relevant to this work. For the positive-energy projection, we employed the "cutting" projector and utilized quadruple precision arithmetic operations. The no-pair DCB approach is currently available only for two-electron systems; however, for two-electron triplet di- and triatomic systems, there is a nonvanishing contribution, which is used as a test case. The no-pair DCB energy includes not only the leadingorder but also high-order $(Z\alpha)^n$ contributions; but, for small Z nuclear charges, these higher-order contributions are small (so, we did not perform any " α " scaling of the variational

4.2.1. Triplet H₂. The two lowest-energy triplet electronic states of the H₂ molecule are labeled as a ${}^3\Sigma_g^+$ and b ${}^3\Sigma_u^+$. For

these states, only the spin-spin matrix elements are nonzero due to spatial symmetry (Table 2). The spin-spin interaction lifts the 3-fold degeneracy of each state, resulting the $\Delta E^{(2)}$ = $E_0^{(2)} - E_{\pm 1}^{(2)}$ zero-field splitting, where the subscript of the energy labels the electron spin angular momentum projection on the body-fixed z axis, fixed to the two nuclei. There are spin-dependent BP computations in the literature for these states, in which the full configuration interaction (FCI) approach was used and reached 1 mEh convergence of the nonrelativistic energy.⁷² In the present work, we converged the nonrelativistic energy with fECGs to 1 μE_h . The computed $\Delta E^{(2)}$ energy splitting agrees with the literature value (precise to 1-2 digits), but our value is more precise (to 3-4 digits). Furthermore, our perturbative BP energy splitting is in excellent agreement with the no-pair DCB splitting. The nopair DCB energy was computed using the same fECG (nonlinear) parametrization as the perturbative computations, and not surprisingly, the two energy splittings converge at a similar pace. Differences appear only at the sub-n E_h (<10⁻⁹ E_h) level, which is well below the finite basis size error (and the range of the leading-order, $\alpha^2 E_h$ relativistic effects).

4.2.2. Triplet H $_3^+$. For the lowest-energy triplet state of H $_3^+$, two nuclear geometries are considered (Table 3). Previous FCI computations ^{73,74} converged the nonrelativistic energy to 10–100 $\mu E_{\rm h}$, but we are not aware of any spin-dependent BP

computations and zero-field splitting values published in the literature.

We report computations using the spin-dependent BP implementation (presented in this work) and verify the results against our existing no-pair DCB approach at two distinct geometries. First, we consider the equilibrium structure, which is linear and has two proton—proton distances equal to $R_{\rm pp,1}$ = $R_{\rm pp,2}$ = 2.454 bohr.⁷³ Due to the triatomic, linear geometry, the 3-fold degeneracy of the energy is lifted into a nondegenerate and a doubly degenerate pair of states with $M_S = 0$ and $M_S =$ ± 1 (where we chose the axis defined by the three nuclei for the quantization axis of the electron spin). Next, we repeated the computation for another, nonlinear geometry (which is near a saddle point⁷⁴ on the potential energy surface) with two proton-proton distances, $R_{pp,1} = 1.939$ bohr, $R_{pp,2} = 5.961$ bohr, and one proton–proton angle $\angle_{ppp} = 64.4^{\circ}$. In this case, the 3-fold degeneracy of the energy is completely lifted; so, we report two energy splittings for the three energy levels in Table 3. The spin-dependent BP implementation is in excellent agreement with the results of the no-pair DCB approach. The latter is currently applicable only for twoelectron systems, so we proceed with the BP implementation for further, poly electronic molecular applications (with two or more clamped nuclei).

5. NUMERICAL APPLICATIONS: HELIUM DIMER

We compute the spin-dependent Breit—Pauli matrix elements connecting electronically excited states of the triplet He₂ molecule (Figure 1). The convergence of the nonrelativistic

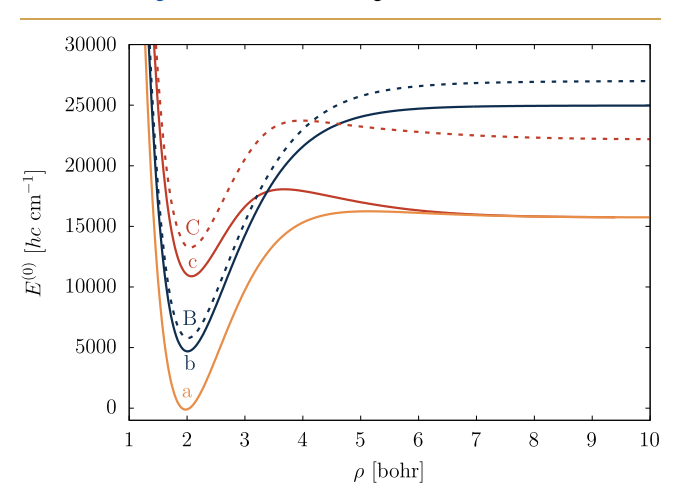


Figure 1. Low-lying excited triplet and singlet states of He₂ studied in this work.

energy at $\rho=2$ bohr (internuclear distance) is reiterated in Table 4; the a $^3\Sigma_u^+$ state basis sets were taken from ref 26 and the b $^3\Pi_g$ and c $^3\Sigma_g^+$ states from ref 27. The B $^1\Pi_g$ and C $^1\Sigma_g^+$ states are computed in this work in order to account for the most important relativistic couplings of the a, b, c subspace. The electronic energy was converged by variational (nonlinear) optimization of the fECG basis functions using the stochastic variational method in combination with the Powell nonlinear optimizer. 9,10,26,64

In what follows, the atomic nuclei are along the (body-fixed) z axis. The z projection of the total, orbital plus electron spin, angular momentum, $\hat{L}_z + \hat{S}_z$ is conserved for clamped nuclei,

and its quantum number is labeled with Ω according to the spectroscopic practice. ⁷⁵ Application of these results in rovibrational and rovibronic computations is reported in ref 26 and also in ref 27.

In the rest of this section, we report the computation of the relativistic (QED) coupling terms and extensively test their convergence with the basis set size. Comparison with earlier computations by Yarkony⁵⁴ is also shown, although the earlier literature results are not well-converged.

5.1. Fine Structure of the a ${}^{3}\Sigma_{11}^{+}$ State

The lowest-energy triplet state of the He₂ molecule is the a $^3\Sigma_{\rm u}^+$ state. The relativistic magnetic spin dipole—dipole interaction, eq 11, lifts the 3-fold degeneracy of this state by splitting it into components with $\Omega=0$ and $\Omega=\pm 1$ (Figure 2). This splitting can be characterized by a single parameter, κ , which is the energy deviation of the $\Omega=0$ state from the centroid. The corresponding shift of the $\Omega=\pm 1$ states is $-\frac{\kappa}{2}$, so the weighted average of the energies equals the centroid energy. The parameter κ has relativistic and QED contributions

$$\kappa = \alpha^2 \kappa^{(2)} + \alpha^3 \kappa^{(3)} \tag{37}$$

Since $\kappa^{(2)}$ originates solely from the relativistic magnetic spin dipolar term (SS,dp), eq 11, its QED correction is obtained by simple multiplication, eq 15

$$\kappa^{(3)} = \frac{1}{\pi} \kappa^{(2)} \tag{38}$$

For the a $^3\Sigma_{\rm u}^+$ state, we think that the nonrelativistic energy is converged to 1–10 $\mu E_{\rm h}$ for the largest basis sets at $\rho=2$ bohr internuclear distance (Table 4). The convergence of $\kappa^{(2)}$ with respect to the number of basis functions is shown in Table 6. For the largest basis sets ($N_{\rm a}=1000-2000$), its value is converged to at least three significant digits. These results agree to one(-two) digit(s) of the multireference configuration interaction (MRCI) computations reported in the literature. The somewhat lower accuracy of the MRCI results is most probably related to the finite basis set error, which we can significantly improve by using an explicitly correlated basis set.

The A $^1\Sigma_{\rm g}^+$ state is closest to the a-state near the equilibrium structure (Figure 1), but there is no direct (first-order) coupling between a and A states through the relativistic (and QED) operators, eq 16. Well, they can couple through second-order effects (some details are collected in the Supporting Information), exploratory computations show that these $\alpha^4E_{\rm h}$ order contributions are tiny (on the few pico-Hartree, p $E_{\rm h}$ level), so the A state is not considered further in this work.

5.2. Fine Structure of the b ${}^3\Pi_{\rm q}$ and c ${}^3\Sigma_{\rm q}^+$ States

The nonvanishing spin-dependent BP matrix elements connecting the b and c states are collected in Table 5. The parameter ε labels the separation (zero-field splitting) of the $M_{\rm S}=0$ and $M_{\rm S}=\pm 1$ states in the c subspace. For the b subspace, the nonzero electron orbital angular momentum introduces a more complicated splitting pattern. It takes three independent parameters, labeled as β , γ_1 , and γ_2 , which describe the shift and splitting of the originally 6-fold degenerate subspace into three 2-fold degenerate states with $\Omega=\pm 2$, $\Omega=\pm 1$, and $\Omega=0$ (Figure 2).

Additionally, the b and c electronic-spin states couple through the matrix elements labeled as δ_1 and δ_2 in Table 6, hence, only the b states for $\Omega=\pm 2$ remain degenerate.

Table 4. He₂ ($\rho = 2$ bohr): The Non-relativistic Energy, $E_x^{(0)}$ in E_h , with Respect to the Number of Optimized fECGs, N_x , for the x = a, b, c, B, and C Electronic States (Figure 1)²¹

a $^3\Sigma_{\mathrm{u}}^+$		$b^{-3}\Pi_{ m g}$			$c^{3}\Sigma_{\mathrm{g}}^{+}$		В $^1\Pi_{ m g}$		$C^{1}\Sigma_{g}^{+}$	
N_{a}	$E_{\rm a}^{(0)}$	N_{b}	$E_{\rm b}^{(0)}$	$N_{\rm c}$	$E_{\rm c}^{(0)}$	$N_{ m B}$	$E_{ m B}^{(0)}$	$N_{\rm C}$	$E_{\rm C}^{(0)}$	
50	-5.1467	50	-5.1242	50	-5.0920	300	-5.12427	300	-5.08938	
100	-5.14996	100	-5.12787	100	-5.0976	500	-5.12438	500	-5.089739	
200	-5.15079	200	-5.128822	300	-5.10000			750	-5.089804	
500	-5.151071	300	-5.128823	500	-5.100315					
1000	-5.151114	500	-5.129246	750	-5.100426					
1500	-5.1511225	750	-5.129307	1000	-5.100465					
2000	-5.1511238	1000	-5.129330	1500	-5.100482					

[&]quot;The "a" state basis set is from ref 26, the "b" and "c" states are from ref 27.

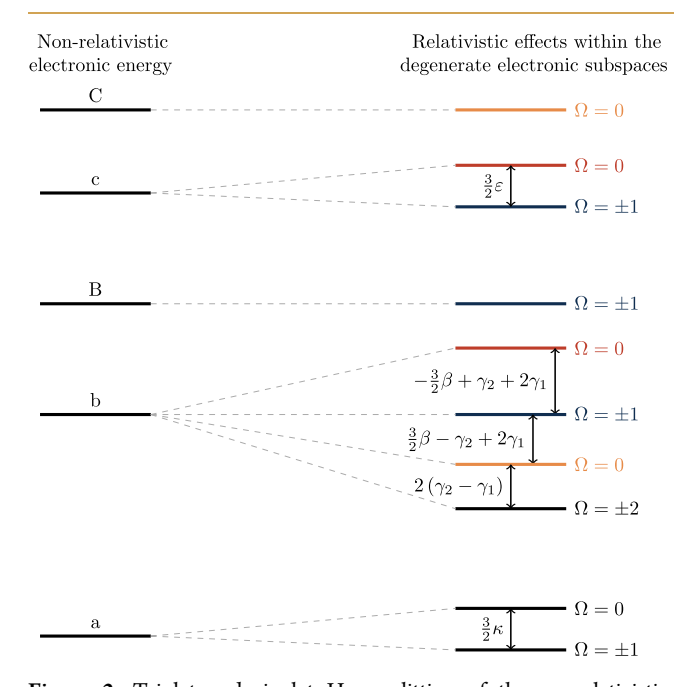


Figure 2. Triplet and singlet He₂: splitting of the nonrelativistic energies degenerate in $M_{\rm S}$ by spin-dependent relativistic (and QED) terms. For the definition of λ , δ_1 , δ_2 , ζ , and ξ please see Table 5 (and ref 27). Color-coding is employed to indicate states that are coupled via relativistic interactions between distinct nondegenerate subspaces (orange: λ , red: δ_2 , blue: δ_1 , ζ , ξ).

Non-negligible couplings also exist with the singlet states, most importantly, with the B $^1\Pi_g$ and the C $^1\Sigma_g^+$ states (Figure 1); the nonvanishing BP matrix elements are labeled with λ , ζ , and ξ in Table 5. Similarly to κ , the relativistic and QED couplings for the parameters β , γ_1 , and ε differ only by a simple multiplicative factor, since only the magnetic spin dipolar term contributes to the relativistic coupling

$$\beta^{(3)} = \frac{1}{\pi} \beta^{(2)}, \qquad \qquad \gamma_1^{(3)} = \frac{1}{\pi} \gamma_1^{(2)}, \qquad \qquad \varepsilon^{(3)} = \frac{1}{\pi} \varepsilon^{(2)}$$
(39)

For the other matrix elements, the QED terms were calculated according to eq 15, and their convergence is shown in Table 7. For matrix elements with the singlet B and C states, due to the smaller basis sets used in this work, the nonrelativistic energies are by 1-2 orders of magnitude less accurate than the a nonrelativistic energy (Table 4). Despite this lower accuracy, the precision of the relativistic and QED couplings appears to be comparable to that of κ , the uncertainties are in the second digit after the decimal point (Tables 6 and 7). To test the convergence, we increased the B and C basis sizes to $N_{\rm B}$ = 500 and $N_{\rm C}$ = 750, respectively, while using the largest b and c basis sets. The resulting changes in the coupling values are in the second to the fourth decimal digits. These results are expected to be sufficiently accurate for the rovibronic computations, primarily focusing on b-c states, as presented in ref 27.

Table 5. Non-vanishing Spin-Dependent Relativistic (and QED) Matrix Elements within the b, c, B, C Electronic-Spin Subspace of He₂^a

	$b^{x,-1}$	$b^{x,0}$	$b^{x,1}$	$b^{y,-1}$	$b^{y,0}$	$b^{y,1}$	c ^{0,-1}	c ^{0,0}	c ^{0,1}	$B^{x,0}$	$B^{y,0}$	C ^{0,0}
$b^{x_{j}-1}$	$-\beta$		$-\gamma_1$	$-i\gamma_2$		$-i\gamma_1$		δ_2				λ
$b^{x,0}$	·	2β	·				$-\delta_1$		δ_1		iζ	·
$b^{x,1}$	$-\gamma_1$	•	$-\beta$	$i\gamma_1$		$i\gamma_2$	•	$-\delta_2$			•	λ
$b^{y,-1}$	$i\gamma_2$	•	$-i\gamma_1$	$-\beta$		γ_1	•	$\mathrm{i}\delta_2$			•	iλ
$b^{y,0}$					2β	•	$\mathrm{i}\delta_1$		$\mathrm{i} \delta_1$	$-\mathrm{i}\zeta$		
$b^{y,1}$	$\mathrm{i}\gamma_1$		$-i\gamma_2$	γ_1		$-\beta$		i δ_2				$-i\lambda$
$c^{0,-1}$		$-\delta_1$			$-\mathrm{i}\delta_1$	•	$-\varepsilon$			ξ	iξ	
$c^{0,0}$	δ_2		$-\delta_2$	$-\mathrm{i}\delta_2$		$-\mathrm{i}\delta_2$		2ε		•		
c ^{0,1}		δ_1			$-\mathrm{i}\delta_1$				$-\varepsilon$	ξ	$-\mathrm{i}\xi$	
$\mathbf{B}^{x,0}$					iζ		ξ		ξ			
$\mathbf{B}^{y,0}$		$-\mathrm{i}\zeta$					-iξ		iξ			
$C^{0,0}$	λ		λ	$-i\lambda$		iλ				•		•

[&]quot;The superscript of each state labels the Cartesian component of the spatial part (as computed in QUANTEN) and the M_S quantum number of the total electron-spin projection on the internuclear axis. The "." labels zero (0) (Further details can be found in the Supplementary Material of ref 27).

Table 6. Convergence of the Relativistic Spin-Dependent Contributions, in mE_h , within the a, b, c, B, and C Electronic-Spin Subspace of He_2 ($\rho = 2 \text{ bohr}$)^a

N_{a}	$N_{ m b}$	$N_{\rm c}$	$\alpha^2 \kappa^{(2)}$	$\alpha^2 \beta^{(2)}$	$lpha^2 \gamma_1^{(2)}$	$\alpha^2 \gamma_2^{(2)}$	$lpha^2 \delta_1^{(2)}$	$\alpha^2 \delta_2^{(2)}$	$\alpha^2 \varepsilon^{(2)}$	$\alpha^2 \lambda^{(2)}$	$\alpha^2 \zeta^{(2)}$	$\alpha^2 \xi^{(2)}$
50	50	50	1.7	-3.19	12.24	20.7	-1.57	-8.68	1.61	-5.735	28.831	10.070
100	100	100	1.9	-3.19	12.43	19.99	-1.24	-8.67	1.65	-5.756	29.606	10.495
200	300	300	2.01	-3.182	12.472	19.69	-1.01	-8.596	1.688	-5.768	29.815	10.764
500	500	500	2.07	-3.1694	12.4671	19.621	-0.931	-8.559	1.6947	-5.768	29.870	10.835
1000	750	750	2.078	-3.1689	12.4691	19.598	-0.914	-8.549	1.6951	-5.764	29.881	10.858
1500	1000	1000	2.081	-3.1687	12.4691	19.586	-0.901	-8.538	1.6946	-5.763	29.883	10.862
2000	1000	1500	2.082	-3.1687	12.4691	19.586	-0.898	-8.537	1.6952	-5.763	29.883	10.866
	1000	1500 ^b								-5.767	29.929	10.874
	et al. ^{52c}		2.01									
Minaev	56 <i>d</i>								2.14			
Yarkony	y ⁵⁴						-1.20	-4.39		-4.359	24.330	10.375
Rosmus	et al. ⁵⁵		2.107	-3.200	12.552	20.62						

 $[^]a\kappa$ corresponds to the zero-field splitting of the "a" state, and Table 5 defines all other non-vanishing matrix elements within the b, c, B, C subspace. $N_{\rm B} = 300$ and $N_{\rm C} = 500$, unless stated otherwise. $^bN_{\rm B} = 500$ and $N_{\rm C} = 750$. $^cR = 2.015$ bohr bond distance for a $^3\Sigma_{\rm u}^+$. $^dR = 2.08$ bohr bond distance for c $^3\Sigma_{\rm g}^+$.

Table 7. Convergence of the Spin-Dependent, Leading-Order QED Contributions, in 0.1 m E_h , within the b, c, B, and C Electronic-Spin Subspace of He₂ (See Also Tables 5 and 6)^a

$N_{ m b}$	$N_{ m c}$	$\alpha^3 \gamma_2^{(3)}$	$lpha^3\delta_1^{(3)}$	$lpha^3\delta_2^{(3)}$	$\alpha^3\lambda^{(3)}$	$\alpha^3 \zeta^{(3)}$	$\alpha^3 \xi^{(3)}$
50	50	0.28	-1.22	-1.13	1.236	-7.66	2.06
100	100	0.02	-1.24	-0.84	1.250	-7.87	2.15
300	300	0.138	-1.511	-0.91	1.261	-7.94	2.221
500	500	0.160	-1.502	-0.925	1.264	-7.951	2.238
750	750	0.168	-1.500	-0.931	1.2630	-7.9551	2.243
1000	1000	0.171	-1.4974	-0.934	1.2626	-7.9560	2.244
1000	1500	0.171	-1.4966	-0.935	1.2626	-7.9560	2.246
1000	1500 ^b				1.2638	-7.9676	2.2453

 $[^]aN_{\rm B}$ = 300 and $N_{\rm C}$ = 500, unless stated otherwise. $\beta^{(3)}$, $\gamma_1^{(3)}$, $\varepsilon^{(3)}$, and $\kappa^{(3)}$ can be calculated from eqs 38 and 39 and Table 6. $^bN_{\rm B}$ = 500 and $N_{\rm C}$ = 750.

6. SUMMARY, CONCLUSION, AND OUTLOOK

In this paper, we reported methodological details and benchmark numerical results for the spin-dependent relativistic and leading-order QED couplings of electronic states of small molecules. The relativistic and QED couplings of the high-precision nonrelativistic electronic states are computed as matrix elements of the spin-dependent operators of the Breit–Pauli Hamiltonian, including the spin—orbit, spin—own—orbit, spin—other—orbit, and spin—spin terms. The corrections due to the electron's anomalous magnetic moment are also accounted for. To accurately describe small polyelectronic molecules, we use a variational floating explicitly correlated Gaussian (fECG) basis procedure.

For small molecular species, accurate and complete fine-structure data are scarcely available, and this work fills this gap. First of all, we tested the methodology for an atomic system, for which (higher precision) fine-structure splitting data are already available in the literature. Then, we computed spin-dependent Breit–Pauli Hamiltonian matrix elements for the two-electron triplet $\rm H_2$ and triplet $\rm H_3^+$. High-precision literature data are not available for these fine-structure splittings; however, for these two-electron systems, we verified the results against our in-house developed no-pair Dirac–Coulomb–Breit (np-DCB) Hamiltonian approach, using the same fECG spatial basis set in the two computations. The two approaches give identical splittings to high precision (the most

stringent, direct comparison would be possible by α -scaling the np-DCB results and comparing the $\alpha^2 E_{\rm h}$ order term).

The spin-dependent Breit–Pauli Hamiltonian matrix elements can be evaluated for (in principle) general poly electronic and poly atomic molecules, whereas our current np-DCB ECG implementation is for two electrons (but automatically includes higher-order $(Z\alpha)^n$ effects).

As to new numerical results with the developed methodology, we converge the relativistic and QED couplings for electronically excited triplet (a $^3\Sigma_{\rm u}^+$, b $^3\Pi_{\rm g}$, and c $^3\Sigma_{\rm g}^+$) and singlet (B $^1\Pi_{\rm g}$, C $^1\Sigma_{\rm g}^+$) states of the four-electron He $_2$ molecule to at least 3–4 significant digits, which significantly improves upon (the scarcely) available data in the literature. These results are computed for a series of nuclear configurations and will be used to compute high-resolution spectra, including modeling the fine structure of the rovibronic transitions in a separate paper.

ASSOCIATED CONTENT

Supporting Information

The Supporting Information is available free of charge at https://pubs.acs.org/doi/10.1021/acsphyschemau.5c00055.

Representation of spin functions with spin-adapted states and spinors: case study for four electrons with $M_S = 0$; higher-order fine-structure corrections from other electronic states (PDF)

AUTHOR INFORMATION

Corresponding Author

Edit Mátyus – MTA-ELTE "Momentum" Molecular Quantum Electro-Dynamics Research Group, Institute of Chemistry, Eötvös Loránd University, Budapest H-1117, Hungary; orcid.org/0000-0001-7298-1707; Email: edit.matyus@ttk.elte.hu

Authors

- Péter Jeszenszki MTA-ELTE "Momentum" Molecular Quantum Electro-Dynamics Research Group, Institute of Chemistry, Eötvös Loránd University, Budapest H-1117, Hungary
- Péter Hollósy MTA-ELTE "Momentum" Molecular Quantum Electro-Dynamics Research Group, Institute of Chemistry, Eötvös Loránd University, Budapest H-1117, Hungary
- Adám Margócsy MTA-ELTE "Momentum" Molecular Quantum Electro-Dynamics Research Group, Institute of Chemistry, Eötvös Loránd University, Budapest H-1117, Hungary

Complete contact information is available at: https://pubs.acs.org/10.1021/acsphyschemau.5c00055

Notes

The authors declare no competing financial interest.

ACKNOWLEDGMENTS

P.J. gratefully acknowledges the support of the János Bolyai Research Scholarship of the Hungarian Academy of Sciences (BO/285/22). We thank the European Research Council (Grant No. 851421) and the Momentum Programme of the Hungarian Academy of Sciences (LP2024-15/2024) for their financial support. We acknowledge DKP for granting us access to the Komondor HPC facility.

REFERENCES

- (1) Sheldon, R. E.; Babij, T. J.; Reeder, S. H.; Hogan, S. D.; Cassidy, D. B. Precision Microwave Spectroscopy of the Positronium 2^3 S₁ \rightarrow 2^3 P₂ Interval. *Phys. Rev. Lett.* **2023**, *131*, 043001.
- (2) Clausen, G.; Scheidegger, S.; Agner, J. A.; Schmutz, H.; Merkt, F. Imaging-Assisted Single-Photon Doppler-Free Laser Spectroscopy and the Ionization Energy of Metastable Triplet Helium. *Phys. Rev. Lett.* **2023**, *131*, 103001.
- (3) Alighanbari, S.; Giri, G. S.; Constantin, F. L.; Korobov, V. I.; Schiller, S. Precise test of quantum electrodynamics and determination of fundamental constants with HD⁺ ions. *Nature* **2020**, *581*, 152
- (4) Patra, S.; Germann, M.; Karr, J.-P.; Haidar, M.; Hilico, L.; Korobov, V. I.; Cozijn, F. M. J.; Eikema, K. S. E.; Ubachs, W.; Koelemeij, J. C. J. Proton-electron mass ratio from laser spectroscopy of HD⁺ at the part-per-trillion level. *Science* **2020**, *369*, 1238–1241.
- (5) Germann, M.; Patra, S.; Karr, J.-P.; Hilico, L.; Korobov, V. I.; Salumbides, E. J.; Eikema, K. S. E.; Ubachs, W.; Koelemeij, J. C. J. Three-body QED test and fifth-force constraint from vibrations and rotations of HD⁺. *Phys. Rev. Res.* **2021**, *3*, L022028.
- (6) Langen, T.; Valtolina, G.; Wang, D.; Ye, J. Quantum state manipulation and cooling of ultracold molecules. *Nat. Phys.* **2024**, *20*, 702–712
- (7) Furey, B. J.; Wu, Z.; Isaza-Monsalve, M.; Walser, S.; Mattivi, E.; Nardi, R.; Schindler, P. Strategies for implementing quantum error correction in molecular rotation. *Quantum* **2024**, *8*, 1578.

- (8) Ruttley, D. K.; Hepworth, T. R.; Guttridge, A.; Cornish, S. L. Long-lived entanglement of molecules in magic-wavelength optical tweezers. *Nature* **2025**, *637*, 827–832.
- (9) Suzuki, Y.; Varga, K. Stochastic Variational Approach to Quantum-Mechanical Few-Body Problems; Springer-Verlag: Berlin, 1998.
- (10) Mitroy, J.; Bubin, S.; Horiuchi, W.; Suzuki, Y.; Adamowicz, L.; Cencek, W.; Szalewicz, K.; Komasa, J.; Blume, D.; Varga, K. Theory and application of explicitly correlated Gaussians. *Rev. Mod. Phys.* **2013**, *85*, 693–749.
- (11) Strasburger, K. High angular momentum states of lithium atom, studied with symmetry-projected explicitly correlated Gaussian lobe functions. *J. Chem. Phys.* **2014**, *141*, 044104.
- (12) Strasburger, K. Explicitly correlated wave functions of the ground state and the lowest quintuplet state of the carbon atom. *Phys. Rev. A* **2019**, 99, 052512.
- (13) Cencek, W. Explicitly Correlated Wave Functions. *Chemistry and Physics: Theory and Applications*; Rychlewski, J., Ed.; Springer Netherlands: Dordrecht, 2003; pp 347–370.
- (14) Pavanello, M.; Adamowicz, L.; Alijah, A.; Zobov, N. F.; Mizus, I. I.; Polyansky, O. L.; Tennyson, J.; Szidarovszky, T.; Császár, A. G. Calibration-quality adiabatic potential energy surfaces for H₃⁺ and its isotopologues. *J. Chem. Phys.* **2012**, *136*, 184303.
- (15) Tung, W.-C.; Pavanello, M.; Adamowicz, L. Very accurate potential energy curve of the He₂⁺ ion. *J. Chem. Phys.* **2012**, *136*, 104309.
- (16) Ferenc, D.; Mátyus, E. Non-adiabatic mass correction for excited states of molecular hydrogen: Improvement for the outer-well HH⁻¹ Σ_o ⁺ term values. *J. Chem. Phys.* **2019**, *151*, 094101.
- (17) Ferenc, D.; Korobov, V. I.; Mátyus, E. Nonadiabatic, Relativistic, and Leading-Order QED Corrections for Rovibrational Intervals of ${}^{4}\text{He2+} (X^{2}\Sigma_{u}^{+})$. *Phys. Rev. Lett.* **2020**, *125*, 213001.
- (18) Patkóš, V.; Yerokhin, V. A.; Pachucki, K. Complete α^7 m Lamb shift of helium triplet states. *Phys. Rev. A* **2021**, *103*, 042809.
- (19) Nasiri, S.; Tumakov, D.; Stanke, M.; Kędziorski, A.; Adamowicz, L.; Bubin, S. Fine structure of the doublet *P* levels of boron. *Phys. Rev. Res.* **2024**, *6*, 043225.
- (20) Ferenc, D.; Jeszenszki, P.; Matyus, E. Variational vs perturbative relativistic energies for small and light atomic and molecular systems. *J. Chem. Phys.* **2022**, *157*, 094113.
- (21) Mátyus, E.; Ferenc, D.; Jeszenszki, P.; Margócsy, A. The Bethe-Salpeter QED Wave Equation for Bound-State Computations of Atoms and Molecules. ACS Phys. Chem. Au 2023, 3, 222.
- (22) Saly, E.; Ferenc, D.; Mátyus, E. Pre-Born-Oppenheimer energies, leading-order relativistic and QED corrections for electronically excited states of molecular hydrogen. *Mol. Phys.* **2023**, *121*, e2163714
- (23) Ferenc, D.; Mátyus, E. Evaluation of the Bethe Logarithm: From Atom to Chemical Reaction. *J. Phys. Chem. A* **2023**, 127, 627–633.
- (24) Ferenc, D.; Mátyus, E. Benchmark potential energy curve for collinear H₃. Chem. Phys. Lett. 2022, 801, 139734.
- (25) Mátyus, E.; Margócsy, A.·. Rovibrational computations for He_2^+ $X\Sigma_u^+$ including non-adiabatic, relativistic and QED corrections. *arXiv* **2025**, arXiv:2506.19120.
- (26) Margócsy, A.; Rácsai, B.; Jeszenszki, P.; Mátyus, E. Rovibrational computations for the He₂ a $^3\Sigma_{\rm u}^+$ state including non-adiabatic, relativistic, and QED corrections. *arXiv* **2025**, arXiv:2506.19116.
- (27) Rácsai, B.; Jeszenszki, P.; Margócsy, Á.; Mátyus, E. High-precision quantum dynamics of He₂ over the b ${}^3\Pi_g$ -c ${}^3\Sigma_g^+$ electronic subspace by including non-adiabatic, relativistic and QED corrections and couplings. *J. Chem. Phys.* **2025**, *163*, 081102.
- (28) Pachucki, K.; Cencek, W.; Komasa, J. On the acceleration of the convergence of singular operators in Gaussian basis sets. *J. Chem. Phys.* **2005**, *122*, 184101.
- (29) Jeszenszki, P.; Ireland, R. T.; Ferenc, D.; Mátyus, E. On the inclusion of cusp effects in expectation values with explicitly correlated Gaussians. *Int. J. Quantum Chem.* **2022**, 122, e26819.

- (30) Rácsai, B.; Ferenc, D.; Margócsy, Á.; Mátyus, E. Regularized relativistic corrections for polyelectronic and polyatomic systems with explicitly correlated Gaussians. *J. Chem. Phys.* **2024**, *160*, 211102.
- (31) Douglas, M.; Kroll, N. M. Quantum electrodynamical corrections to the fine structure of helium. *Ann. Phys.* **1974**, *82*, 89–155.
- (32) Patkóš, V.; Yerokhin, V. A.; Pachucki, K. Two-body *P*-state energies at order α^6 . *Phys. Rev. A* **2024**, *109*, 022819.
- (33) Yerokhin, V. A.; Patkóš, V.; Puchalski, M.; Pachucki, K. QED calculation of ionization energies of 1*snd* states in helium. *Phys. Rev. A* **2020**, *102*, 012807.
- (34) Yerokhin, V. A.; Patkóš, V.; Pachucki, K. Atomic Structure Calculations of Helium with Correlated Exponential Functions. *Symmetry* **2021**, *13*, 1246.
- (35) Bergeson, S. D.; Balakrishnan, A.; Baldwin, K. G. H.; Lucatorto, T. B.; Marangos, J. P.; McIlrath, T. J.; O'Brian, T. R.; Rolston, S. L.; Sansonetti, C. J.; Wen, J.; Westbrook, N.; Cheng, C. H.; Eyler, E. E. Measurement of the He Ground State Lamb Shift via the Two-Photon 1¹S 2¹S Transition. *Phys. Rev. Lett.* **1998**, *80*, 3475–3478.
- (36) Kandula, D. Z.; Gohle, C.; Pinkert, T. J.; Ubachs, W.; Eikema, K. S. E. XUV frequency-comb metrology on the ground state of helium. *Phys. Rev. A* **2011**, *84*, 062512.
- (37) Clausen, G.; Jansen, P.; Scheidegger, S.; Agner, J. A.; Schmutz, H.; Merkt, F. Ionization Energy of the Metastable 2 ¹S₀ State of ⁴He from Rydberg-Series Extrapolation. *Phys. Rev. Lett.* **2021**, *127*, 093001.
- (38) Clausen, G.; Merkt, F. Ionization Energy of Metastable 3 He (2 S₁) and the Alpha- and Helion-Particle Charge-Radius Difference from Precision Spectroscopy of the *np* Rydberg Series. *Phys. Rev. Lett.* **2025**, 134, 223001.
- (39) Puchalski, M.; Komasa, J.; Pachucki, K. Fine and hyperfine splitting of the low-lying states of Be⁹. Phys. Rev. A 2021, 104, 022824.
- (40) Kędziorski, A.; Stanke, M.; Adamowicz, L. Atomic fine-structure calculations performed with a finite-nuclear-mass approach and with all-electron explicitly correlated Gaussian functions. *Chem. Phys. Lett.* **2020**, *751*, 137476.
- (41) Stanke, M.; Kędziorski, A.; Adamowicz, L. Fine structure of the beryllium ³P states calculated with all-electron explicitly correlated Gaussian functions. *Phys. Rev. A* **2022**, *105*, 012813.
- (42) Yerokhin, V. A.; Patkóš, V. c. v.; Pachucki, K. QED calculations of energy levels of heliumlike ions with $5 \le Z \le 30$. *Phys. Rev. A* **2022**, 106, 022815.
- (43) Nasiri, S.; Bubin, S.; Adamowicz, L. Isotopic shifts in ³P states of the carbon atom. *Mol. Phys.* **2024**, *122*, e2325049.
- (44) Korobov, V. I.; Hilico, L.; Karr, J.-P. Hyperfine structure in the hydrogen molecular ion. *Phys. Rev. A* **2006**, *74*, 040502.
- (45) Haidar, M.; Korobov, V. I.; Hilico, L.; Karr, J.-P. Higher-order corrections to spin-orbit and spin-spin tensor interactions in hydrogen molecular ions: Theory and application to H₂⁺. *Phys. Rev. A* **2022**, *106*, 022816.
- (46) Haidar, M.; Korobov, V. I.; Hilico, L.; Karr, J.-P. Higher-order corrections to the spin-orbit and spin-spin tensor interactions in HD⁺. *Phys. Rev. A* **2022**, *106*, 042815.
- (47) Nasiri, S.; Bubin, S.; Adamowicz, L. Non-Born—Oppenheimer Electronic Structure and Relativistic Effects in the Ground States of BH and BH⁺. *J. Phys. Chem. A* **2025**, *129*, 1623–1633.
- (48) Jeszenszki, P.; Mátyus, E. Relativistic two-electron atomic and molecular energies using LS coupling and double groups: Role of the triplet contributions to singlet states. *J. Chem. Phys.* **2023**, *158*, 054104.
- (49) Holdener, M.; Wirth, V.; Shahin, N. A.; Beyer, M.; Merkt, F. Characterization of the electronic ground state of He₂⁺ by high-resolution photoelectron spectroscopy. *Phys. Rev. A* **2025**, *112*, 022815.
- (50) Wirth, V.; Holdener, M.; Merkt, F. Precision Spectroscopy of the Fine Structure in the $a^3\Sigma_{\rm u}^{\ +}(\nu=0)$ and $c^3\Sigma_{\rm g}^{\ +}(\nu=4)$ States of the Helium Dimer. *Phys. Rev. A* **2025**, *112*, 032807.
- (51) Verdegay, L.; Zeng, B.; Knapp, D. Y.; Roth, J. C.; Beyer, M. Laser cooling Rydberg molecules a detailed study of the helium dimer. *New J. Phys.* **2025**, 27, 093201.

- (52) Beck, D. R.; Nicolaides, C. A.; Musher, J. I. Calculation of the fine structure of the a ${}^{3}\Sigma u+$ state of molecular helium. *Phys. Rev. A* **1974**, 10, 1522–1527.
- (53) Chabalowski, C. F.; Jensen, J. O.; Yarkony, D. R.; Lengsfield, B. H. Theoretical study of the radiative lifetime for the spin-forbidden transition $a^3\Sigma_{u+} \to X^{-1}\Sigma_g^{+}$ in He₂. *J. Chem. Phys.* **1989**, *90*, 2504–2512.
- (54) Yarkony, D. R. On the quenching of helium 2^3S : Potential energy curves for, and nonadiabatic, relativistic, and radiative couplings between, the ${}^3\Sigma_{\rm u}{}^+$, A ${}^1\Sigma_{\rm u}{}^+$, b ${}^3\Pi_{\rm g}$, B ${}^1\Pi_{\rm g}$, c ${}^3\Sigma_{\rm g}{}^+$, and C ${}^1\Sigma_{\rm g}{}^+$ states of He₂. *J. Chem. Phys.* **1989**, 90, 7164–7175.
- (55) Bjerre, N.; Mitrushenkov, A. O.; Palmieri, P.; Rosmus, P. Spinorbit and spin-spin couplings in He₂ and He₂. *Theor. Chem. Acc.* **1998**, *100*, 51–59.
- (56) Minaev, B. Fine structure and radiative lifetime of the low-lying triplet states of the helium excimer. *Phys. Chem. Chem. Phys.* **2003**, *5*, 2314–2319.
- (57) Nijjar, P.; Krylov, A. I.; Prezhdo, O. V.; Vilesov, A. F.; Wittig, C. Triplet Excitons in Small Helium Clusters. *J. Phys. Chem. A* **2019**, *123*, 6113–6122.
- (58) Xu, S.; Lu, A.; Zhong, X.; Guo, Y.; Shi, J. Ab initio investigation of potential energy curves of He_2 , He_2^+ , and extrapolation by the machine learning method. *Int. J. Quantum Chem.* **2024**, *124*, e27367.
- (59) Dyall, K. G.; Faegri, K., Jr. Introduction to Relativistic Quantum Chemistry; Oxford University Press: New York, 2007.
- (60) Reiher, M.; Wolf, A. Relativistic Quantum Chemistry: The Fundamental Theory of Molecular Science, 2nd ed.; Wiley-VCH: Weinheim, 2015.
- (61) Schwinger, J. On Quantum-Electrodynamics and the Magnetic Moment of the Electron. *Phys. Rev.* **1948**, *73*, 416–417.
- (62) Sucher, J. Energy Levels of the Two-Electron Atom, to Order α^3 Rydberg. PhD Dissertation, Columbia University, 1958.
- (63) Jentschura, U. D.; Adkins, G. S. Quantum Electrodynamics: Atoms, Lasers and Gravity; World Scientific: Singapore, 2022.
- (64) Mátyus, E.; Reiher, M. Molecular Structure Calculations: a Unified Quantum Mechanical Description of Electrons and Nuclei using Explicitly Correlated Gaussian Functions and the Global Vector Representation. *J. Chem. Phys.* **2012**, *137*, 024104.
- (65) Mátyus, E. Pre-Born—Oppenheimer molecular structure theory. *Mol. Phys.* **2019**, *117*, 590—609.
- (66) Jeszenszki, P.; Ferenc, D.; Mátyus, E. All-order explicitly correlated relativistic computations for atoms and molecules. *J. Chem. Phys.* **2021**, *154*, 224110.
- (67) Jeszenszki, P.; Ferenc, D.; Mátyus, E. Variational Dirac—Coulomb explicitly correlated computations for atoms and molecules. *J. Chem. Phys.* **2022**, *156*, 084111.
- (68) Ferenc, D.; Jeszenszki, P.; Mátyus, E. On the Breit interaction in an explicitly correlated variational Dirac-Coulomb framework. *J. Chem. Phys.* **2022**, *156*, 084110.
- (69) Mohr, P. J.; Newell, D. B.; Taylor, B. N.; Tiesinga, E. CODATA recommended values of the fundamental physical constants: 2022. *Rev. Mod. Phys.* 2025, *97*, 025002.
- (70) Hollósy, P.; Jeszenszki, P.; Mátyus, E. One-Particle Operator Representation over Two-Particle Basis Sets for Relativistic QED Computations. J. Chem. Theory Comput. 2024, 20, 5122–5132.
- (71) Nonn, A.; Margócsy, A.; Mátyus, E. Bound-State Relativistic Quantum Electrodynamics: A Perspective for Precision Physics with Atoms and Molecules. *J. Chem. Theory Comput.* **2024**, *20*, 4385–4395.
- (72) Minaev, B.; Loboda, O.; Rinkevicius, Z.; Vahtras, O.; Ågren, H. Fine and hyperfine structure in three low-lying ${}^3\Sigma^+$ states of molecular hydrogen. *Mol. Phys.* **2003**, *101*, 2335–2346.
- (73) Sanz, C.; Roncero, O.; Tablero, C.; Aguado, A.; Paniagua, M. The lowest triplet state A_3 of H_3^+ : Global potential energy surface and vibrational calculations. *J. Chem. Phys.* **2001**, *114*, 2182–2191.
- (74) Cernei, M.; Alijah, A.; Varandas, A. J. C. Accurate double many-body expansion potential energy surface for triplet H_3^+ . I. The lowest adiabatic sheet (a ${}^3\Sigma u+$). *J. Chem. Phys.* **2003**, *118*, 2637–2646.
- (75) Lefebvre-Brion, H.; Field, R. W. The Spectra and Dynamics of Diatomic Molecules; Academic Press, 2004.